J|A|C|S
ARTICLES
Published on Web 03/03/2007

Characterization and Mechanism of Formation of Tandem Lesions in DNA by a Nucleobase Peroxyl Radical

In Seok Hong, K. Nolan Carter, Kousuke Sato, and Marc M. Greenberg*

Department of Chemistry, Johns Hopkins University, 3400 North Charles Street, Baltimore, Maryland 21218

Received January 2, 2007; E-mail: mgreenberg@jhu.edu

Abstract: 5,6-Dihydro-2′-deoxyuridin-6-yl (**1**) was independently generated via photolysis of **3**. The radical is an analogue of the major reactive species produced from thymidine upon reaction with hydroxyl radical, which is the dominant DNA-damaging agent produced by the indirect effect of γ-radiolysis. Under aerobic conditions, the peroxyl radical (**2**) derived from **1** reacts ~82% of the time with either the 5′- or 3′-adjacent nucleotide to produce two contiguously damaged nucleotides, known as tandem lesions. The structures and distribution of tandem lesions were investigated using probes that selectively detect abasic sites, ESI-MS/MS, and competition kinetics. In addition to 2-deoxyribonolactone, nonoxidized abasic sites were detected. ^{18}O-Labeling verified that H_2O was the source of oxygen in the abasic sites, but that O_2 was the source of the oxygen in the 5,6-dihydro-6-hydroxy-2′-deoxyuridine derived from **2**. ESI-MS/MS experiments, in conjunction with isotopic labeling, identified several products and provided direct evidence for peroxyl radical addition to the adjacent thymine bases. Kinetic studies revealed that peroxyl radical addition to the 5′-thymine was favored by ~4−5-fold over C1′-hydrogen atom abstraction from the respective deoxyribose ring, and that 2-deoxyribonolactone formation accounts for ~11% of the total amount of tandem lesions produced. These results suggest that tandem lesions, whose biochemical effects are largely unknown, constitute a major family of DNA damage products produced by the indirect effect of γ-radiolysis.

Introduction

Reactive oxygen species are produced in cells by endogenous processes and exogenous reagents, such as γ-radiolysis, which is the most common nonsurgical cancer treatment.[1,2] DNA is an important biological molecule that is attacked by reactive oxygen species, particularly hydroxyl radical (OH•). Nucleobase radicals resulting from π-bond addition of the diffusible species are the major family of reactive intermediates produced when nucleic acids react with OH•.[1] Nucleobase radicals are believed to account for as much as 90% of the reactions with OH•. The nucleobase radicals are also formed from hydration of cation radicals, following direct ionization of the biopolymer. Multiple reaction pathways are available to nucleobase radicals. For instance, quenching of the nucleobase radicals by reactants typically present in cells, such as thiols and/or O_2 gives rise to modified nucleotides. These lesions include molecules such as 8-hydroxy-7,8-dihydro-2′-deoxyguanosine and thymine glycol, which are mutagenic and/or cytotoxic if not repaired.[3−7]

Strand cleavage is another consequence of nucleic acid oxidation that is important to genomic stability. Consequently, significant attention has been paid to the ability of nucleobase radicals to induce strand breaks. In order to result in strand scission a nucleobase radical or its respective peroxyl radical must abstract a hydrogen atom from the biopolymer's carbohydrate backbone. Radiolysis experiments suggest that as much as 40% and 5% of the reactions between OH• and RNA or DNA, respectively, result in direct strand scission.[8,9] These and other studies indicate that one or more pathways exist for transferring the spin from the base to the sugar. By using techniques such as EPR spectroscopy and mass spectrometry to observe the reactive intermediates and their products, respectively,[10−12] a great deal has been learned about the reactivity of randomly generated nucleobase radicals generated by γ-radiolysis and other oxidants. Since 1995 chemists have studied radical-mediated DNA damage by independently generating deoxyribose and nucleobase radicals in oligonucleotides from nonnative, photolabile nucleosides.[13−16] This approach has enabled unam-

(1) Von Sonntag, C. *Free-Radical-Induced DNA Damage and Its Repair*; Springer-Verlag: Berlin, 2006.
(2) Halliwell, B.; Gutteridge, J. M. C. *Free Radicals in Biology and Medicine*, 3rd ed.; Oxford Science Publications: Oxford, 1999.
(3) Ide, H.; Kow, Y. W.; Wallace, S. S. *Nucleic Acids Res.* **1985**, *13*, 8035−8052.
(4) Basu, A. K.; Loechler, E. L.; Leadon, S. A.; Essigmann, J. M. *Proc. Natl. Acad. Sci. U.S.A.* **1989**, *86*, 7677−7681.
(5) Wood, M. L.; Basu, A. K.; Essigmann, J. M. *UCLA Symp. Mol. Cell. Biol., New Ser.* **1990**, *136*, 201−209.
(6) Wood, M. L.; Esteve, A.; Morningstar, M. L.; Kuziemko, G. M.; Essigmann, J. M. *Nucleic Acids Res.* **1992**, *20*, 6023−6032.
(7) Neeley, W. L.; Essigmann, J. M. *Chem. Res. Toxicol.* **2006**, *19*, 491−505.
(8) Lemaire, D. G. E.; Bothe, E.; Schulte-Frohlinde, D. *Int. J. Radiat. Biol.* **1984**, *45*, 351−358.
(9) Milligan, J. R.; Aguilera, J. A.; Nguyen, T.-T. D. *Radiat. Res.* **1999**, *151*, 334−342.
(10) Sevilla, M. D.; Becker, D. *Electron Paramagn. Reson.* **2004**, *19*, 243−278.
(11) Bernhard, W. A.; Mroczka, N.; Barnes, J. *Int. J. Radiat. Biol.* **1994**, *66*, 491−497.
(12) Dizdaroglu, M.; Jaruga, P.; Birincioglu, M.; Rodriguez, H. *Free Rad. Biol. Med.* **2002**, *32*, 1102−1115.
(13) Giese, B.; Beyrich-Graf, X.; Erdmann, P.; Giraud, L.; Imwindelried, P.; Müller, S. N.; Schwitter, U. *J. Am. Chem. Soc.* **1995**, *117*, 6146−6147.

Scheme 1. Generation of 5,6-Dihydro-2′-deoxyuridin-6-yl Radical (**1**)

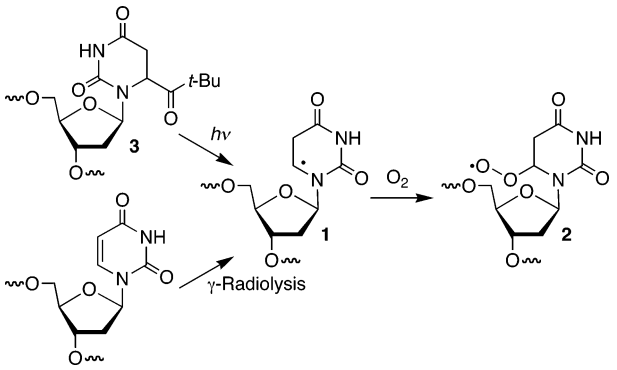

biguous characterization of nucleobase radical reactivity in DNA by incorporating precursors site specifically in chemically synthesized oligonucleotides. Independent generation of DNA radicals has uncovered novel DNA damage pathways, such as the formation of tandem lesions from dihydropyrimidine peroxyl radicals. Herein we provide product characterization and mechanistic substantiation for the complex set of DNA tandem lesions derived from 5,6-dihydro-2′-deoxyuridin-6-yl (**1**, Scheme 1), which is a member of the major family of radiolytically produced reactive intermediates.

Tandem lesions are defined as two contiguously damaged nucleotides within DNA. They are a subset of clustered lesions, which comprise two lesions within one to two turns of DNA, irrespective of which strand they are in. There is considerable interest in clustered lesions because they can inhibit DNA repair and/or ultimately give rise to increased levels of double-strand breaks.[17−20] In general, clustered lesions are formed by multiple oxidation events when DNA is exposed to γ-radiolysis.[21−23] However, tandem lesions can also form via reaction between a nucleotide radical and an adjacent nucleotide. Amplifying a single DNA oxidation event to form a product that is potentially more deleterious to the cell than an isolated lesion is biologically significant and potentially appealing from the standpoint of designing DNA-damaging agents. Tandem lesions have been characterized in DNA samples following exposure to ionizing radiation.[24−28] Independent generation of reactive intermediates has provided a direct link between specific tandem lesions and radical intermediates.[29−35] In one instance, this approach uncovered the first example of a nucleotide radical that produces interstrand cross-links by reacting with the opposing nucleobase.[36,37] We also found that nucleobase peroxyl radicals react with adjacent nucleotides by adding to the respective nucleobase and by abstracting hydrogen atoms from the deoxyribose.[14,38,39]

More recently, we determined that tandem lesions were the major products derived from 5,6-dihydro-2′-deoxyuridin-6-yl's (**1**) respective peroxyl radical (**2**, Scheme 1).[40−42] 5,6-Dihydro-2′-deoxyuridin-6-yl (**1**) is a model of the major hydroxyl radical adduct of thymidine (**4**) and was chosen because of the synthetic expediency of the Norrish type I photochemical precursor (**3**).[41] Initial studies established that **2** added to the pyrimidine nucleobase and abstracted the C1′-hydrogen atom from the 5′-adjacent nucleotide in duplex DNA (**5**, **6**).[40] However, the constraints imposed by the right-handed helix prevented hydrogen atom abstraction from the 2′-deoxyribose of the 3′-adjacent nucleotide. Independent generation of **1** at a defined site within the DNA enabled the use of structural modifications at the proximal nucleotides to establish that 6*R*-**2** and 6*S*-**2** produced tandem lesions at the 5′- and 3′-adjacent nucleotides via their respective *syn*- and *anti*-conformational isomers, because glycosidic bond rotation was competitive with the reaction rate constants of the diastereomeric peroxyl radicals.[42] We now describe experiments that utilize new methods for selectively detecting abasic lesions in DNA, and we provide the first mass spectrometric evidence for tandem lesions containing a peroxide linkage between damaged nucleotides. These and kinetic competition experiments provide a more complete mechanistic description of radical-mediated tandem lesion formation from **2**.

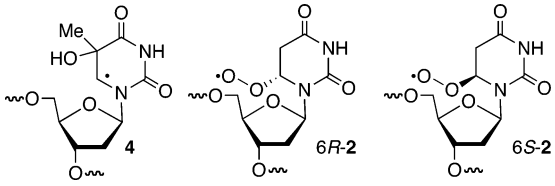

Results and Discussion

Chemoselective Abasic Site Detection. Photolysis of **3** in duplex DNA (5′-^{32}P-**5**, -**6**) produces alkali-labile lesions that are cleaved upon NaOH treatment (0.1 M, 37 °C, 20 min) at the nucleotide where the radical is generated and the 5′-adjacent nucleotide. Cleavage under such mild conditions is consistent

(14) Barvian, M. R.; Greenberg, M. M. *J. Am. Chem. Soc.* **1995**, *117*, 8291−8292.
(15) Greenberg, M. M. *DNA and Aspects of Molecular Biology*; Kool, E. T., Ed.; Comprehensive Natural Products Chemistry, Vol. 7; Elsevier: Amsterdam, 1999; pp 371−426.
(16) Greenberg, M. M. *Chem. Res. Toxicol.* **1998**, *11*, 1235−1248.
(17) Gulston, M.; de Lara, C.; Jenner, T.; Davis, E.; O'Neill, P. *Nucleic Acids Res.* **2004**, *32*, 1602−1609.
(18) David-Cordonnier, M. H.; Boiteux, S.; O'Neill, P. *Biochemistry* **2001**, *40*, 11811−11818.
(19) David-Cordonnier, M. H.; Laval, J.; O'Neill, P. *Biochemistry* **2001**, *40*, 5738−5746.
(20) Weinfeld, M.; ResouliNia, A.; Chaudhry, M. A.; Britten, R. A. *Radiat. Res.* **2001**, *156*, 584−589.
(21) Brenner, D. J.; Ward, J. F. *Int. J. Radiat. Biol.* **1992**, *61*, 737−748.
(22) Gulston, M.; Fulford, J.; Jenner, T.; de Lara, C.; O'Neill, P. *Nucl. Acids Res.* **2002**, *30*, 3464−3472.
(23) Sutherland, B. M.; Bennett, P. V.; Sutherland, J. C.; Laval, J. *Radiat. Res.* **2002**, *157*, 611−616.
(24) Box, H. C.; Patrzyc, H. B.; Dawidzik, J. B.; Wallace, J. C.; Freund, H. G.; Iijima, H.; Budzinski, E. E. *Radiat. Res.* **2000**, *153*, 442−446.
(25) Box, H. C.; Budzinski, E. E.; Dawidzik, J.; Patrzyc, H. B.; Freund, H. G. *Radiat. Res.* **2001**, *156*, 215−219.
(26) Bellon, S.; Ravanat, J.-L.; Gasparutto, D.; Cadet, J. *Chem. Res Toxicol.* **2002**, *15*, 598−606.
(27) Bourdat, A.-G.; Douki, T.; Frelon, S.; Gasparutto, D.; Cadet, J. *J. Am. Chem Soc.* **2000**, *122*, 4549−4556.
(28) Douki, T.; Riviere, J.; Cadet, J. *Chem. Res. Toxicol.* **2002**, *15*, 445−454.
(29) Zhang, Q.; Wang, Y. *J. Am. Chem. Soc.* **2004**, *126*, 13287−13297.
(30) Hong, H.; Wang, Y. *J. Am. Chem. Soc.* **2005**, *127*, 13969−13977.
(31) Zhang, Q.; Wang, Y. *Chem. Res. Toxicol.* **2005**, *18*, 1897−1906.
(32) Zhang, Q.; Wang, Y. *J. Am. Chem. Soc.* **2003**, *125*, 12795−12802.
(33) Liu, Z.; Gao, Y.; Wang, Y. *Nucleic Acids Res.* **2003**, *31*, 5413−5424.
(34) Romieu, A.; Bellon, S.; Gasparutto, D.; Cadet, J. *Org. Lett.* **2000**, *2*, 1085−1088.
(35) Zhang, Q.; Wang, Y. *Nucleic Acids Res.* **2005**, *33*, 1593−1603.
(36) Hong, I. S.; Ding, H.; Greenberg, M. M. *J. Am. Chem. Soc.* **2006**, *128*, 485−491.
(37) Hong, I. S.; Greenberg, M. M. *J. Am. Chem. Soc.* **2005**, *127*, 3692−3693.
(38) Tallman, K. A.; Greenberg, M. M. *J. Am. Chem. Soc.* **2001**, *123*, 5181−5187.
(39) Greenberg, M. M.; Barvian, M. R.; Cook, G. P.; Goodman, B. K.; Matray, T. J.; Tronche, C.; Venkatesan, H. *J. Am. Chem. Soc.* **1997**, *119*, 1828−1839.
(40) Carter, K. N.; Greenberg, M. M. *J. Am. Chem. Soc.* **2003**, *125*, 13376−13378.
(41) Carter, K. N.; Greenberg, M. M. *J. Org. Chem.* **2003**, *68*, 4275−4280.
(42) Hong, I. S.; Carter, K. N.; Greenberg, M. M. *J. Org. Chem.* **2004**, *69*, 6974−6978.

Scheme 2. Selective Detection of 2-Deoxyribonolactone

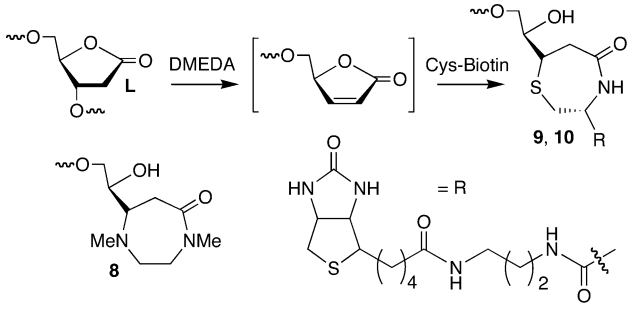

with the formation of abasic sites.[43−45] Reaction with the deoxyribose of the 3′-adjacent nucleotide is not observed due to the relative inaccessibility of the corresponding hydrogen atoms. Chemical fingerprinting following generation of **1** in **5** and **6**, and MALDI-TOF MS analysis of products produced in **7** confirmed that 2-deoxyribonolactone (L) was formed at the 5′-adjacent nucleotide as part of a tandem lesion. However, these experiments did not enable us to determine the structure of the abasic site at the nucleotide position where the radical is originally generated, nor did they establish that 2-deoxyribonolactone was the exclusive abasic lesion produced at the 5′-adjacent nucleotide.

5′-d(GAG CTA GCT CGA CC**X**$_{15}$ **3**T$_{17}$A GGA CCT GCA GCT)
3′-d(CTC GAT CGA GCT GGA AA T CCT GGA CGT CGA)
5 X = thymidine (T)
6 X = 5,6-dihydrothymidine (dHT)

5′-d(TAT CCT **3**TA CTA)
7

A more complete description of 2-deoxyribonolactone (L) formation was obtained using a probe (Cys-Biotin) that selectively detects this oxidized abasic lesion (Scheme 2). The C4′-oxidized abasic (C4-AP) lesion does not react with Cys-Biotin, and the nonoxidized abasic (AP) lesion forms an adduct that decomposes under the heating conditions used in the assay.[46] Adducts consistent with Cys-Biotin trapping of the β-elimination

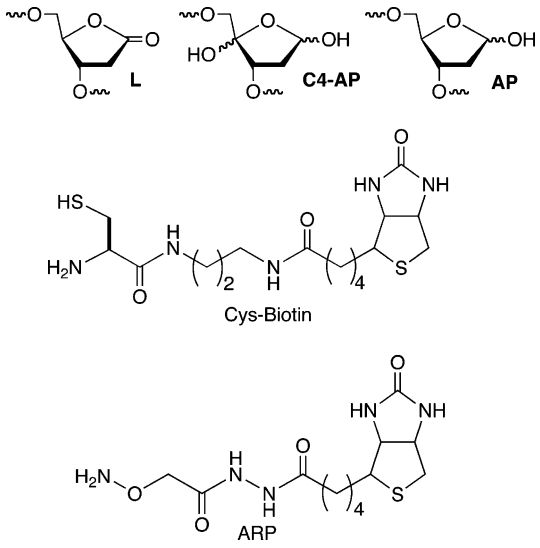

product from L at the 5′-adjacent nucleotide (**9**, Scheme 2, Figure 1) were detected in photolysates of 5′-^{32}P-**5** and 5′-^{32}P-**6**. The retarded migration and heat lability of the adducts are consistent with their previous characterization.[46,47] The larger amounts of adduct detected in the 5,6-dihydrothymidine (dHT)-containing duplex are consistent with the previously proposed partitioning of **2** between C1′-hydrogen atom abstraction and nucleobase addition.[40,42] Saturation of the 5′-adjacent thymine ring in 5′-^{32}P-**6** shifts more of the reactivity of **2** to the deoxyribose. A characteristic adduct between *N*,*N*′-dimethylethylenediamine (DMEDA), which is used to form the butenolide elimination product (Scheme 2) is also observed (**8**, Scheme 2, Figure 1).[46,47] In addition, Cys-Biotin treatment of 5′-^{32}P-**5** gives rise to a slower moving product (**10**, Figure 1) that is consistent with L formation at the nucleotide where **2** is originally generated. The photolyzed duplex (5′-^{32}P-**6**) containing dHT also forms a Cys-Biotin adduct at the original site of the nucleotide, but most of this product is decomposed upon heating, indicating that AP lesions account for the majority of these labile sites.[46] Hence, this experiment reveals that the majority of the NaOH-labile product produced at the position where **1** is produced in **6** is an AP site, and only small amounts of L are present.

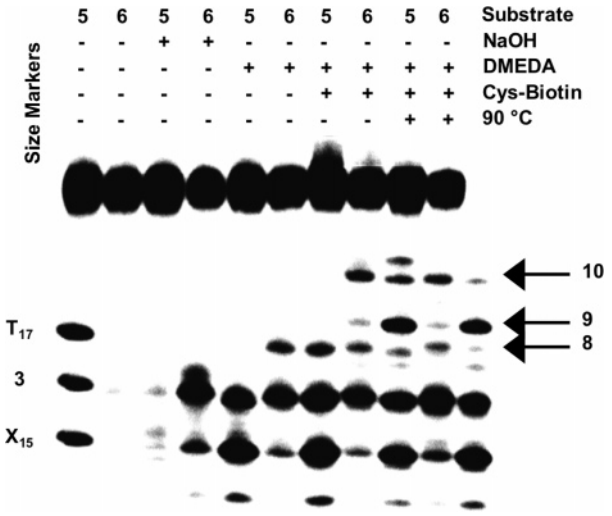

Figure 1. Phosphorimage illustrating 2-deoxyribonolactone (L) detection using Cys-Biotin.

AP site formation was directly probed for by taking advantage of commercially available aldehyde reactive probe (ARP). ARP reacts with AP sites, including C4-AP, but not 2-deoxyribonolactone (L).[46,48,49] However, formation of the C4-AP lesion was ruled out on the basis of the absence of the distinctive product formed upon reaction with hydrazine (data not shown).[50] Unlike Cys-Biotin, the DNA remains intact after ARP reaction with AP. Although the ARP-adducted oligonucleotide migrates slightly more slowly through a denaturing polyacrylamide gel, it was difficult to separate from large amounts of nonadducted oligonucleotide. Consequently, the photolyzed substrates (3′-

(43) Roupioz, Y.; Lhomme, J.; Kotera, M. *J. Am. Chem. Soc.* **2002**, *124*, 9129−9135.
(44) Zheng, Y.; Sheppard, T. L. *Chem. Res. Toxicol.* **2004**, *17*, 197−207.
(45) Kim, J.; Gil, J. M.; Greenberg, M. M. *Angew. Chem., Int. Ed.* **2003**, *42*, 5882−5885.
(46) Sato, K.; Greenberg, M. M. *J. Am. Chem. Soc.* **2005**, *127*, 2806−2807.
(47) Hwang, J.-T.; Tallman, K. A.; Greenberg, M. M. *Nucleic Acids Res.* **1999**, *27*, 3805−3810.
(48) Xue, L.; Greenberg, M. M. *Angew. Chem., Int. Ed.* **2007**, *46*, 561−564.
(49) Jeong, Y. C.; Sangaiah, R.; Nakamura, J.; Pachkowski, B. F.; Ranasinghe, A.; Gold, A.; Ball, L. M.; Swenberg, J. A. *Chem. Res. Toxicol.* **2005**, *18*, 51−60.
(50) Sugiyama, H.; Kawabata, H.; Fujiwara, T.; Dannoue, Y.; Saito, I. *J. Am. Chem. Soc.* **1990**, *112*, 5252−5257.

Scheme 3. Method for Detecting Abasic Sites (AP) by Gel Electrophoresis

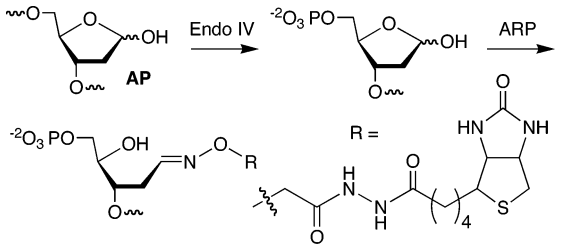

^{32}P-**5**, -**6**) were digested with excess endonuclease IV (Endo IV) prior to treatment with ARP in order to detect AP site formation by polyacrylamide gel electrophoresis (Scheme 3). We did not anticipate any discrimination by Endo IV for the different possible abasic sites, because the enzyme efficiently incises AP and oxidized abasic lesions by hydrolyzing their respective 5′-phosphates, and it was used in excess of the DNA.[51−53] Indeed, Endo IV treatment of photolyzed 3′-^{32}P-**5** and -**6** produces comparable amounts of cleavage, as does NaOH (Figure 2a). A single adduct (**11**, Figure 2a) is observed when Endo IV-digested 3′-^{32}P-**5** is treated with ARP. The product comigrated with the one produced when a comparable duplex (3′-^{32}P-**13**) containing an AP site (independently generated from

5'-d(GAG CTA GCT CGA CCT$_{15}$ **AP**T$_{17}$A GGA CCT GCA GCT)
3'-d(CTC GAT CGA GCT GGA A A T CCT GGA CGT CGA)
13

2′-deoxyuridine by uracil DNA glycosylase at the respective nucleotide position corresponding to the site where **2** is originally generated) is subjected to this protocol (Figure 2b). A more slowly migrating product that would correlate with the ARP adduct at the 5′-adjacent nucleotide in **5** is not detected. This is consistent with the above Cys-Biotin experiments (Figure 1), which indicated AP formation at the original site of radical generation in **5**, but not at the 5′-adjacent nucleotide. In contrast, subjecting photolyzed 3′-^{32}P-**6** to these reaction conditions indicated that AP sites are produced at the site where **2** is generated and at the 5′-adjacent nucleotide (**12**, Figure 2a). Adventitious hydrolysis of the 5,6-dihydrothymidine is not the source of the AP site. The pathway by which the AP site is produced is unknown at this time and is not biologically significant because it is unlikely that a nucleobase radical (e.g., **2**) would be generated adjacent to a 5,6-dihydropyrimidine nucleotide.

The formation of AP from the nucleotide where **2** is produced is mechanistically significant. We speculate that hydrolysis of the glycosidic bond occurs in conjunction with superoxide elimination from **2** (Scheme 4). Superoxide loss from the C6-position of a nucleobase is precedented.[1] Admittedly, the concomitant loss of a proton from N1 of the base must facilitate this reaction, suggesting that the analogous reaction from **2** proceeds with a slower rate constant. In addition, although we were unable to detect superoxide elimination from monomeric **2**, the peroxyl radical is produced at lower concentrations in the polymer (10−20 nM).[41] Hence, radical−radical reactions, which may have precluded detecting superoxide elimination from monomeric **2**, are less likely to compete under these conditions.

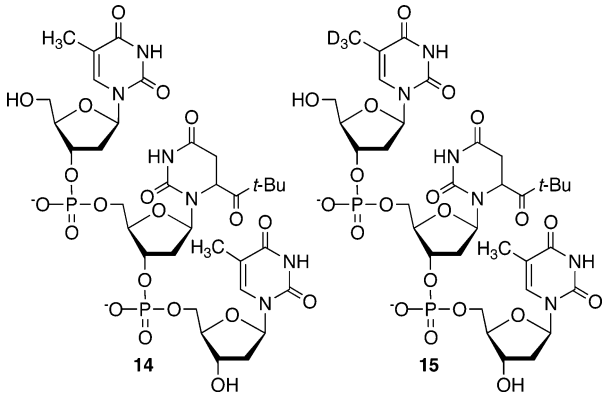

Product Analysis by ESI-MS. MALDI-TOF MS analysis of photolyses of single-stranded substrate containing **3** provided direct evidence for several lesions derived from **2**.[40] In order to provide additional information regarding the reactivity of **2**, we carried out a series of ESI-MS/MS experiments on photolyzed trinucleotides **14** and **15**. The former was photolyzed in the presence of $^{16}O_2$ and $^{18}O_2$. The trideuterated compound (**15**) was used to assist in distinguishing between reactions that occurred between **2** and the 5′- or 3′-adjacent nucleotides.

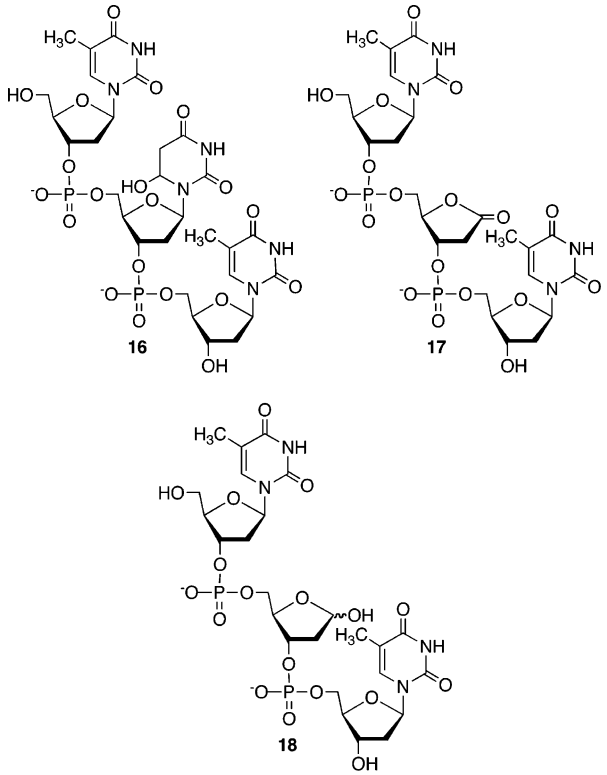

Lesions that solely involve the original radical site included the reduction product of **2** (**16**), and those containing L (**17**) or AP (**18**).[54] The fragmentation pattern of **16** observed upon MS/MS analysis confirmed that 5,6-dihydro-6-hydroxy-2′-deoxyuridine (the C6-hydrate) was derived from the original site of **2**. This was evident by the loss of thymidine residues. In

(51) Bailly, V.; Verly, W. G. *Biochem. J.* **1989**, *259*, 761−768.
(52) Greenberg, M. M.; Weledji, Y. N.; Kim, J.; Bales, B. C. *Biochemistry* **2004**, *43*, 8178−8183.
(53) Greenberg, M. M.; Weledji, Y. N.; Kroeger, K. M.; Kim, J. *Biochemistry* **2004**, *43*, 15217−15222.

(54) See Supporting Information.

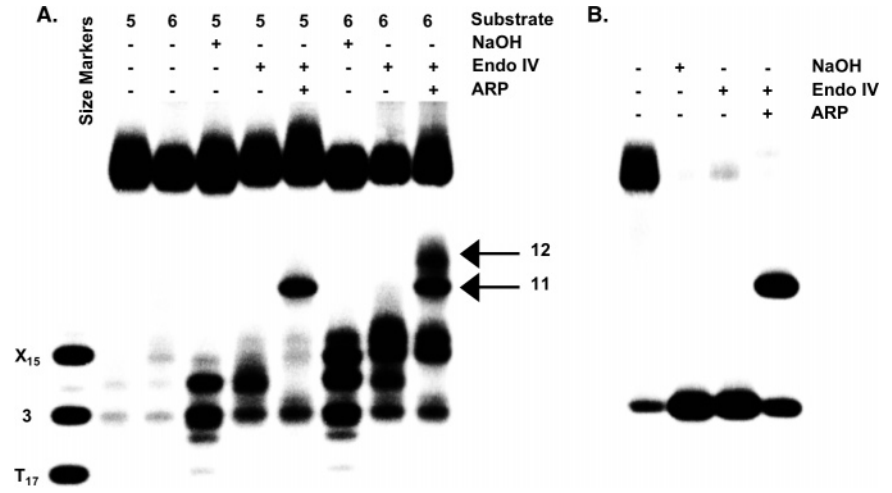

Figure 2. Phosphorimage illustrating AP detection using Endo IV and ARP. (A) AP detection in photolyzed 3′-^{32}P-**5**, -**6**. (B) AP detection in duplex (3′-^{32}P-**13**) containing an independently generated abasic lesion.

Scheme 4. AP Formation from a C6-Peroxyl Radical (**2**)

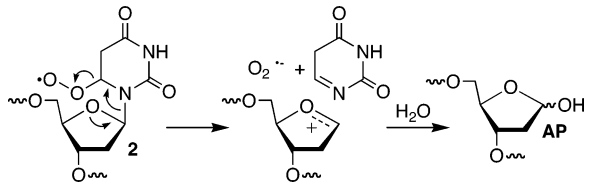

addition, ^{18}O-labeling indicated that the oxygen in the C6-hydrate of **16** was derived from $^{18}O_2$ and that exchange did not occur rapidly with solvent under these conditions.[55] These same techniques verified that the abasic sites were also derived from the nucleotide where the peroxyl radical was produced and that water serves as the source of the oxygen atoms in L (**17**) and AP (**18**).[54] Although we cannot rule out exchange in **17** and **18**, the absence of ^{18}O in these products is consistent with their derivation from ionic intermediates proposed here (Scheme 4) and elsewhere.[56,57]

A variety of tandem lesions (e.g., **19**−**23**) were also identified in the photolysates.[54] Lesions containing fragmented nucleobases

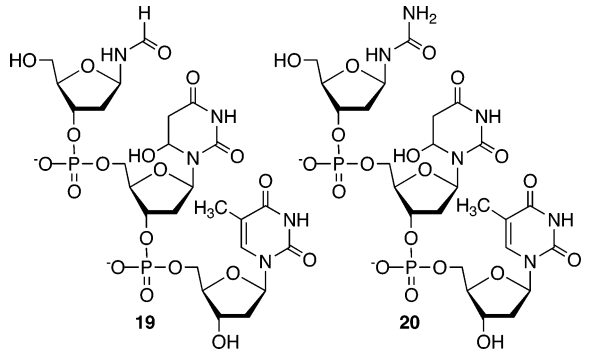

are typically ascribed to decomposition of intermediate oxyl radicals.[1] In this system, the requisite oxyl radicals would result from peroxyl radical addition of **2** into the π-bond of the adjacent thymine rings (Scheme 5 and see below).[40] Products

Scheme 5. Tandem Lesion Formation via Peroxyl Radical Addition to a Nucleobase

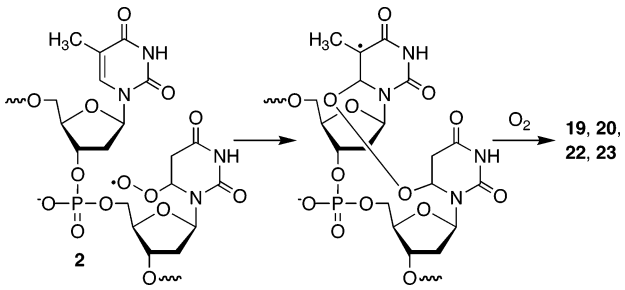

21−**23** were of particular mechanistic import. Isotopic labeling was invaluable in these experiments. In each instance ^{18}O-labeling supported O_2 trapping of **1**, as evidenced by the incorporation of ^{18}O in the nucleotide where the radical is initially generated (Figures 3−5 and Supporting Information). Furthermore, the absence of ^{18}O in the 2-deoxyribonolactone (L) component of **21** was consistent with the proposed superoxide release mechanism for formation of the oxidized abasic lesion (Figure 3).[56,57] Desymmetrization of the trinucleotide via deuterium labeling (**15**) also contributed to structural determination. For instance, the absence of the trideuterated thymine in the MS of irradiated **15** confirms that lactone formation occurs selectively at the 5′-adjacent nucleotide (Figure 3c).

The lesion containing thymine glycol and the C6-hydrate of 2′-deoxyuridine (**22**) is consistent with the proposed pathway involving addition of **2** into the thymine double bond of an adjacent nucleotide (Figure 4). ^{18}O-Labeling revealed that all three oxygen atoms were derived from O_2, as evidenced by the 6 amu increase in the parent ion (Figure 4b). Ions attributable to fragmentation of the dihydropyrimidine rings were also evident. These too were consistent with ^{18}O incorporation at the appropriate C5 and C6 positions of the trinucleotide. The previous reports describing tandem lesion formation from **2** described products resulting from addition to the double bond of the 5′- and 3′-adjacent nucleotides.[40,42] Irradiation of the trideuterated substrate (**15**) verified that tandem lesions containing thymine glycol were formed at both adjacent nucleotides (**22b**, **22c**). This was evident from the fragmentation pattern (Figure 4c) in which pairs of ions differing by 3 amu were

(55) Carter, K. N.; Greenberg, M. M. *Bioorg. Med. Chem.* **2001**, *9*, 2341−2346.
(56) Tallman, K. A.; Tronche, C.; Yoo, D. J.; Greenberg, M. M. *J. Am. Chem. Soc.* **1998**, *120*, 4903−4909.
(57) Emanuel, C. J.; Newcomb, M.; Ferreri, C.; Chatgilialoglu, C. *J. Am. Chem Soc.* **1999**, *121*, 2927−2928.

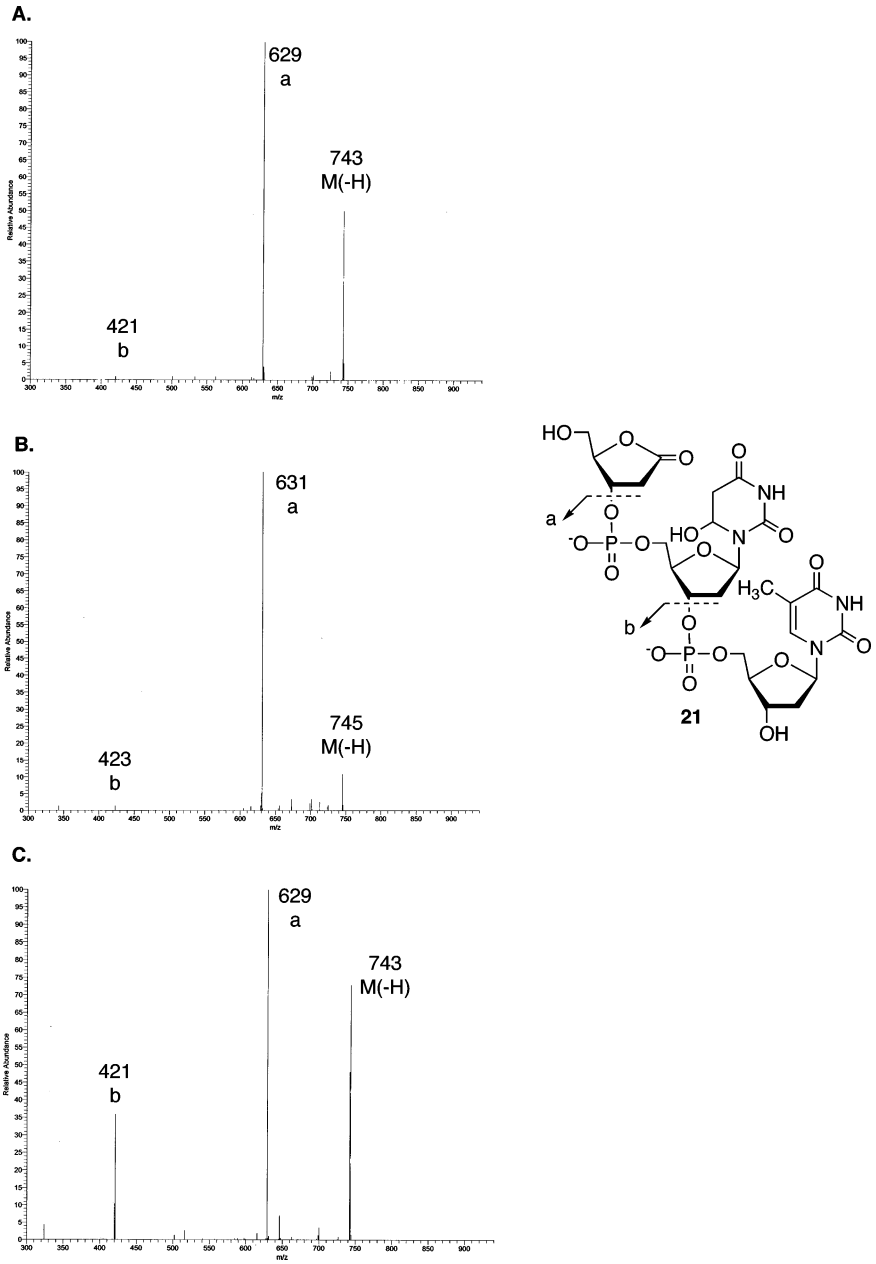

Figure 3. ESI-MS/MS of **21** from (A) photolysis of **14**, (B) photolysis of **14** in $^{18}O_2$, (C) photolysis of **15**.

detected. For instance, fragmentation of the thymine glycol ring to leave only the glycosidic nitrogen atom gave rise to ions with $m/z = 744$ or 747 (c, c′ in Figure 4c) depending upon whether the glycol was present at the 5′-adjacent thymidine (deuterated) or 3′-adjacent nucleotide, respectively. A similar pairing was observed when the thymine glycol ring fragmented so as to retain the C6-carbon and its pendant hydroxyl group (b, b′ in Figure 4c).

Direct support for the formation of lesions such as **22** via addition of **2** to the double bond of thymine (Scheme 5) was obtained by the detection of a peroxide product (**23**, Figure 5). This product was 2 amu lower than the thymine glycol-containing tandem lesion (**22**, Figure 4), which presumably arises from reduction of **23**. The fragmentation pattern of the peroxide (**23**) was similar to that described above for the glycol-containing tandem lesion, except that the respective ions were all 2 amu lower. There was no evidence that the peroxide linkage survived fragmentation of either dihydropyrimidine ring. Additional analogy to **22** was evident in the photolysis carried out in $^{18}O_2$, where it was clear that all three oxygen atoms were derived from O_2 (Figure 5b). Finally, use of the trideuterated substrate (**15**) revealed similar pairings of ions separated by 3 amu, supporting formation of the regioisomeric peroxides (**23b**, **23c**, Figure 5c).

Reaction of 5,6-Dihydro-2′-deoxyuridin-6-yl (1) with Thiols. The rate constants for thiol trapping of 5,6-dihydro-2′-deoxyuridin-6-yl (**1**) were determined by examining the competition for the radical with O_2 (Scheme 6). Trapping by O_2 produces the C6-hydrate (6OH) upon reduction of the peroxyl radical (**2**) by thiol, whereas 5,6-dihydro-2′-deoxyuridine (dHU) is formed by thiol trapping of **1**. The contribution of each trapping pathway was determined by measuring the amount of piperidine-labile products formed as a function of mercaptan concentration. The trapping products' differing

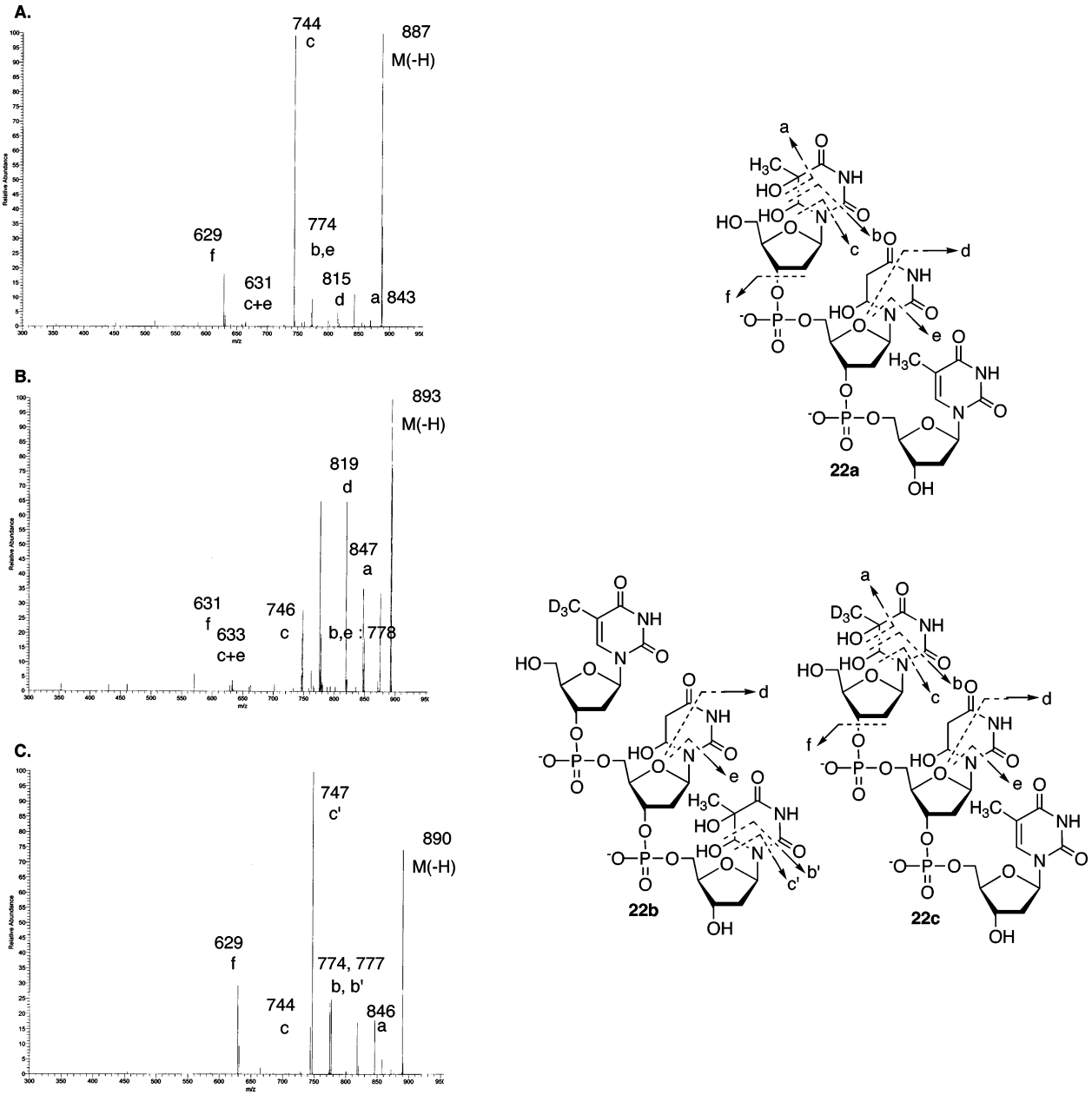

Figure 4. ESI-MS/MS of **22** from (A) photolysis of **14**, (B) photolysis of **14** in $^{18}O_2$, (C) photolysis of **15**.

stability to piperidine was exploited when determining their relative amounts. Piperidine (1.0 M, 90 °C, 20 min) does not cleave oligonucleotides containing the radical precursor or dHU. Hence, the amount of piperidine-induced cleavage is attributed to products resulting from formation of the peroxyl radical (**2**). The amount of dHU was determined by subtracting the percentage of cleaved DNA produced in the presence of thiol from the amount of cleaved product produced in the absence of thiol. Since all measurements relied upon the amount of piperidine cleavage in the absence of thiol, six such samples were prepared and analyzed in each experiment. Samples containing thiol were carried out in triplicate at each concentration used. These experiments were carried out at sufficiently high thiol concentrations (30−500 mM), such that the production of tandem lesions, whose formation kinetics are described below, was not competitive. Other assumptions inherent in these experiments are that the rate constant for radical trapping by O_2 ($k_{O2} = 2 \times 10^9$ M^{-1} s^{-1}) is independent of DNA secondary structure, and that the photochemical conversion of **3** is independent of thiol concentration. In addition, the observed decrease in alkali-labile cleavage as a function of thiol concentration is attributed solely to dHU formation. These assumptions are consistent with previous observations made during the photolyses of monomeric **3**.[41]

The rate constant (Table 1) for β-mercaptoethanol (BME) trapping of **1** in single-stranded DNA (5′-^{32}P-**24**) was within

5'-d(GAG CTA GCT CGA CC**X**$_{15}$ **3**T$_{17}$A GGA CCT GCA GCT)

24

experimental error of that measured in the same manner for the monomeric species ($8.8 \pm 0.5 \times 10^6$ M^{-1} s^{-1}).[41] In addition, the rate constants describing reactions between **1** in DNA and

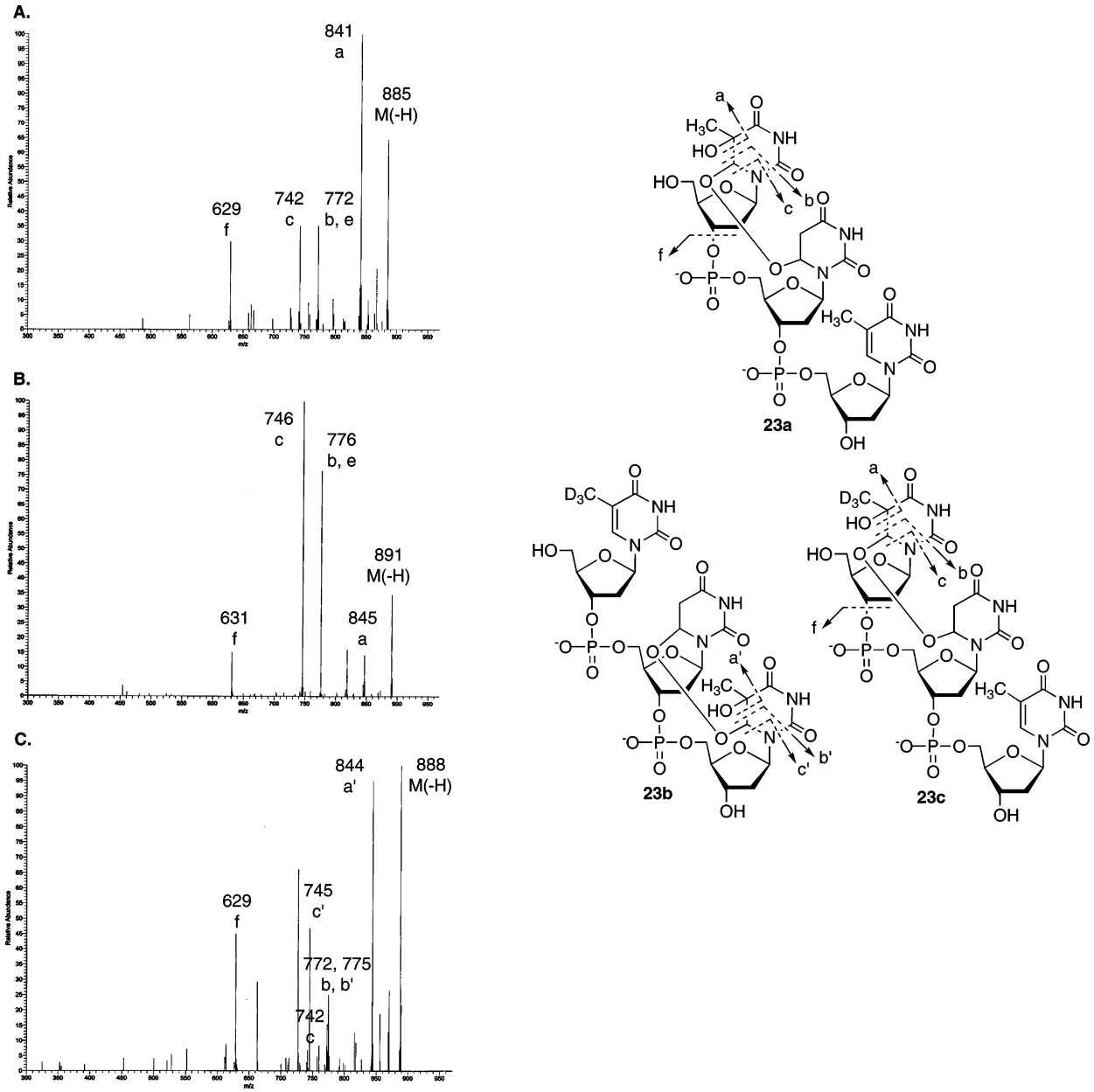

Figure 5. ESI-MS/MS of **23** from (A) photolysis of **14**, (B) photolysis of **14** in $^{18}O_2$, (C) photolysis of **15**.

Table 1. Rate Constants for Reaction of 5,6-Diydro-2′-deoxyuridin-6-yl (**1**) with Thiols in Single-Stranded or Double-Stranded DNA

	k_{RSH} (10^6 $M^{-1}s^{-1}$)	
RSH	single stranded	double stranded
GSH	9.8 ± 0.3	11.9 ± 0.5
BME	8.4 ± 0.3	10.1 ± 0.6

glutathione (GSH) or BME were consistent with those measured for **25**.[36,58] 5,6-Dihydro-2′-deoxyuridin-6-yl (**1**) is trapped in **24** by BME approximately twice as fast as **25** is in single-stranded DNA. The more rapid reactivity of **1** can be rationalized on the basis of the greater radical stabilization by two heteroatom substituents in **25**. The reactivity trend observed for reaction of **1** with thiols in single-stranded versus double-stranded DNA is distinct from that of **25**. A modest (∼20%) increase in rate constants was observed for reaction with each thiol in duplex

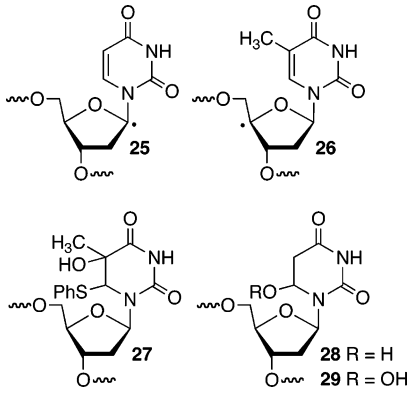

versus single-stranded DNA. In contrast, BME trapping of the C1′-radical derived from 2′-deoxyuridine (**25**) was 4-fold lower in duplex DNA compared to a single-stranded oligonucleotide.[58]

(58) Hwang, J.-T.; Greenberg, M. M. *J. Am. Chem. Soc.* **1999**, *121*, 4311−4315.

Scheme 6. Competitive Trapping of O_2 and Thiol for **1**

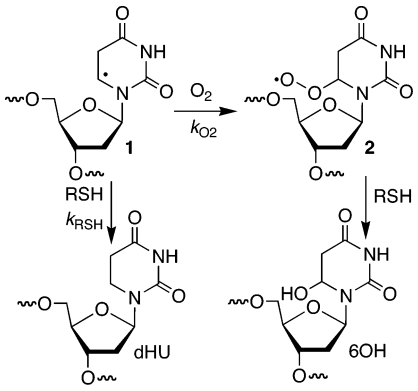

$$\frac{dHU}{6OH} = \frac{k_{RSH}[\mathbf{1}][RSH]}{k_{O2}[\mathbf{1}][O_2]} = \frac{k_{RSH}[RSH]}{k_{O2}[O_2]}$$

The latter result was consistent with the inaccessibility of the C1′-radical in duplex DNA, whereas hybridization was not expected to affect accessibility of the C6-radical.[59] Nucleobase radical **1** also reacted ~4−6 times more rapidly with GSH in a single-stranded substrate than did the C4′-radical produced from thymidine (**26**).[60] There is no obvious explanation for this difference based upon radical stability. It is possible that the different competition methods used may have played a role in approximating the rate constants.

Kinetic Analysis of Tandem Lesion Formation. Measuring the dependency of alkali-labile lesion formation on glutathione concentration allowed us to approximate the rate constants for reaction of **2** with the 5′- and 3′-adjacent nucleotides, and in an intranucleotidyl manner. The yield of direct strand scission was negligible, and is included in the cleavage observed upon alkali treatment.[40] Tandem lesions derived from **1** were not expected to compete with O_2 trapping of the radical. Although these types of lesions were detected in di- and trinucleotides, their yields in dodecameric duplexes were negligible when **4** was generated from **27** under anaerobic conditions.[29,31] A kinetic scheme was constructed that provided four pathways for alkali-labile lesion formation from **2** (Scheme 7). C1′-Intramolecular hydrogen atom abstraction ultimately produces 2-deoxyribonolactone (L), which will be detected as an alkali induced (NaOH or piperidine) cleavage band following polyacrylamide gel electrophoresis (PAGE) separation at the original radical site (**I**).[41,47,56,57] As discussed above, AP lesions may result from **2** via an ionic mechanism (Scheme 4). The rate constant (k_{Intra}) for intranucleotidyl alkali-labile lesion formation represents the sum total of these processes. Thiol trapping (k_{RSH}) of **2** produces the hydroperoxide (**29**), and C6-hydrate (**28**) upon further reduction. These products are cleaved by piperidine. Tandem lesions result from reaction of **2** at either the sugar or base of the 5′- ($k_{5'}$), or the base of the 3′-adjacent ($k_{3'}$) nucleotide. Mild (0.1 M, NaOH, 37 °C) treatment reveals sugar lesions, whereas both families of products are cleaved by piperidine. Because the nucleotide product(s) (e.g., **28**, **29**) at the site of the original radical in each tandem lesion is also alkali-labile, only the tandem lesions involving the nucleotide on the side of the radical precursor that is closer to the radiolabel are independently detected in a single experiment (Scheme 8). The other tandem lesion is detected as part of the cleavage at the original radical site. Hence, 5′- and 3′-tandem lesions were independently detected using 5′-^{32}P-**5** (Figure 6) and 3′-^{32}P-**5** (Figure 7), respectively. The rate constants for tandem lesion formation at the 5′-adjacent nucleotide ($k_{5'}$) and 3′-adjacent nucleotide ($k_{3'}$) were obtained from the slopes of the corresponding plots of internucleotidyl versus intranucleotidyl cleavage as a function of thiol concentration, assuming that GSH traps **2** with the same bimolecular rate constant determined in pulse radiolysis studies ($k_{Trap} = 2 \times 10^2$ M^{-1} s^{-1}) using DNA (Table 2).[61] The rate constant for tandem lesion formation at the 3′-adjacent nucleotide ($k_{3'}$) was obtained using 3′-^{32}P-**5** (Figure 7), and $k_{5'}$ was determined using 5′-^{32}P-**5** (Figure 6). The maximum GSH concentration used in these experiments (0.2 mM) was sufficiently low so as to not compete with O_2 for **1**. The rate constants for internucleotidyl reaction (tandem lesion formation, $k_{5'}$ and $k_{3'}$) were then used to extract the rate constant for intranucleotidyl lesion formation (k_{Intra}) from the respective *y*-intercepts. The values of k_{Intra} measured using 5′- or 3′-^{32}P-**5** were within experimental error of one another (Table 2). Using the average of these measurements for k_{Intra} and the average rate constants for 5′- ($k_{5'}$) and 3′-tandem lesion formation ($k_{3'}$), we estimate that 82% of **2** gives rise to tandem lesions. This is an upper limit for the amount of **2** that produces tandem lesions because it assumes that all lesions produced at

Scheme 7. Kinetic Analysis of Tandem Lesion Formation

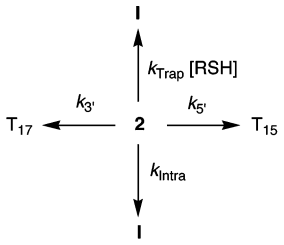

I : Cleavage at original radical site

*3′-^{32}P-**5** :*

$$\frac{[\text{Intra- + 5'-Cleavage}]}{[\text{3'-Cleavage}]} = \frac{\mathbf{I}}{T_{17}} = \frac{k_{5'}[\mathbf{2}] + k_{Intra}[\mathbf{2}] + k_{Trap}[RSH][\mathbf{2}]}{k_{3'}[\mathbf{2}]}$$

$$= \frac{k_{5'} + k_{Intra} + k_{Trap}[RSH]}{k_{3'}} = \frac{k_{5'} + k_{Intra}}{k_{3'}} + \frac{k_{Trap}}{k_{3'}}[RSH]$$

*5′-^{32}P-**5** :*

$$\frac{[\text{Intra- + 3'-Cleavage}]}{[\text{5'-Cleavage}]} = \frac{\mathbf{I}}{T_{15}} = \frac{k_{3'}[\mathbf{2}] + k_{Intra}[\mathbf{2}] + k_{Trap}[RSH][\mathbf{2}]}{k_{5'}[\mathbf{2}]}$$

$$= \frac{k_{3'} + k_{Intra} + k_{Trap}[RSH]}{k_{5'}} = \frac{k_{3'} + k_{Intra}}{k_{5'}} + \frac{k_{Trap}}{k_{5'}}[RSH]$$

Scheme 8. Fragments Observable by Denaturing Gel Electrophoresis upon Alkali Treatment

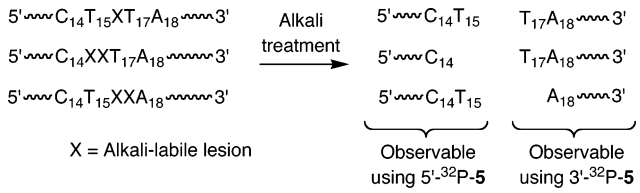

(59) Miaskiewicz, K.; Osman, R. *J. Am. Chem. Soc.* **1994**, *116*, 232−238.
(60) Dussy, A.; Meggers, E.; Giese, B. *J. Am. Chem. Soc.* **1998**, *120*, 7399−7403.
(61) Hildenbrand, K.; Schulte-Frohlinde, D. *Int. J. Radiat. Biol.* **1997**, *71*, 377−385.

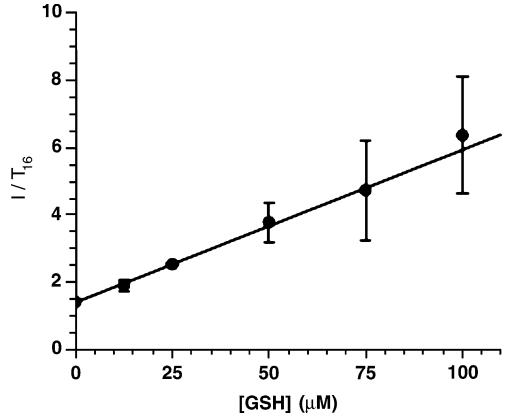

Figure 6. Plot of the amount of alkali-labile cleavage at the position where **2** is generated (I) relative to that at T_{15} as a function of GSH concentration in 5′-^{32}P-**5**.

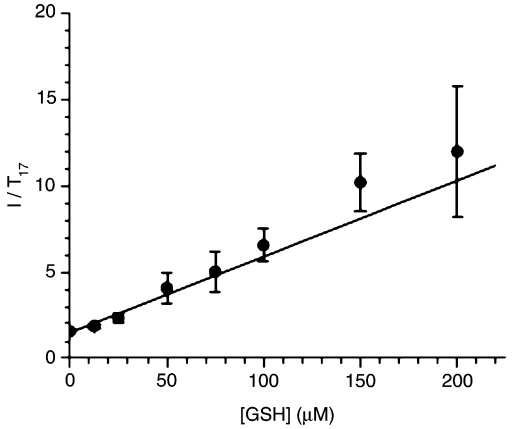

Figure 7. Plot of the amount of alkali-labile cleavage at the position where **2** is generated (I) relative to that at T_{17} as a function of GSH concentration in 3′-^{32}P-**5**.

Table 2. First-Order Rate Constants (s^{-1}) for Intranucleotidyl and Internucleotidyl Reactions of the Peroxyl Radical (**2**) Derived from 5,6-Diydro-2′-deoxyuridin-6-yl (**1**) in Double-Stranded DNA (**5**)

rate constant	(s^{-1})
$k_{5'}$	$4.4 \pm 0.6 \times 10^{-3}$
$k_{3'}$	$4.5 \pm 0.5 \times 10^{-3}$
k_{Intra} (5′-^{32}P-**5**)	$1.7 \pm 0.9 \times 10^{-3}$
k_{Intra} (3′-^{32}P-**5**)	$2.2 \pm 0.4 \times 10^{-3}$

the flanking nucleotides (T_{15}, T_{17}) are components of tandem lesions. A lower limit of 65% tandem lesion formation was previously reported.[40]

Information on the partitioning of reactions between **2** and the 5′-adjacent nucleotide (T_{15}) was obtained by determining the ratio of sugar lesions (NaOH cleavable lesions) at T_{15} and the site at which **2** is generated (Figure 8). As expected, the yields of these products depend upon GSH concentration. As GSH concentration increases, a greater amount of **2** is trapped to form the piperidine (not NaOH)-labile 6OH. Figure 8 reveals that the ratio of NaOH-labile products at T_{15} and the site at which **2** is produced (**I**) is independent of GSH concentration. This suggests that 2-deoxyribonolactone (L) and AP sites are

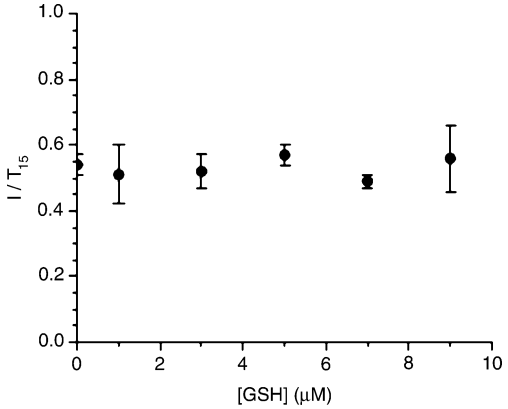

Figure 8. Plot of the amount of sugar lesions (NaOH-labile cleavage) at the position where **2** is generated (I) relative to that at T_{15} as a function of GSH concentration in 5′-^{32}P-**5**.

produced from the peroxyl radical (**2**) and is consistent with the suggestion that the latter is formed by the heterolytic mechanism put forth in Scheme 4. Using the value for k_{Intra} obtained from measurements using 5′-^{32}P-**5** we estimate that the rate constant for the reaction of **2** with the sugar of the 5′-adjacent nucleotide (T_{15}) is $\sim 1 \times 10^{-3}$ s^{-1}. This indicates that 2-deoxyribonolactone formation accounts for ~22% of the reactions between **2** and T_{15}.

Conclusions

Although nucleobase radicals are the major family of reactive intermediates formed when DNA is exposed to γ-radiolysis, this study affirms that one member, 5,6-dihydro-2′-deoxyuridin-6-yl (**1**), does not give rise to direct strand breaks. Instead, the major pathway involves the formation of a peroxyl radical (**2**), which then reacts as much as 82% of the time with either the 5′- or 3′-adjacent nucleotide to form tandem lesions. The majority of the tandem lesions result from addition of **2** to the π-bond of the adjacent pyrimidine. ESI-MS experiments directly support this process, as evidenced by ^{18}O-labeling and the observation of a peroxide product that cross-links the nucleobases of the tandem lesion. Other reports indicate that nucleotide peroxyl radical addition is not limited to adjacent pyrimidines.[27,28] These results suggest that tandem lesions comprise a significant component of DNA damage resulting from reaction with diffusible species. Much less is known about the bypass and repair of tandem lesions than those of isolated ones, but their prevalence suggests that they merit further biochemical characterization.

Acknowledgment. We are grateful for support of this research by the National Institute of General Medical Sciences (GM-054996).

Supporting Information Available: General experimental procedures; ESI-MS of trinucleotides photoproducts **16**−**20**. This material is available free of charge via the Internet at http://pubs.acs.org.

JA0692276